Journal of the European Ceramic Society 19 (1999) 489–496

PII: S0955-2219(98)00219-2
0955-2219/99/$—see front matter

Synthesis, Formation and Characterisation of $FeNbO_4$ Powders

Supon Ananta, Rik Brydson and Noel W. Thomas*

Department of Materials, University of Leeds, Leeds, LS2 9JT, UK

(Received 1 July 1998; accepted 19 September 1998)

Abstract

A modified mixed oxide synthetic route has been developed for the synthesis of iron niobate, $FeNbO_4$ (FN). A rapid vibro-milling technique was employed, with the formation of $FeNbO_4$ phases investigated as a function of calcination temperature and dwell time by XRD and DTA. The particle size distribution of the calcined powder was determined by laser diffraction techniques, and the morphology, phase composition and crystal structure determined via SEM, TEM and EDX. It has been found that the unreacted Fe_2O_3 and $FeNb_2O_6$ phases tend to form together with $FeNbO_4$, with the latter appearing in both monoclinic and orthorhombic phases, depending on calcination conditions. It is seen that optimisation of calcination conditions can lead to a 100% yield of $FeNbO_4$ in an orthorhombic, α-PbO_2-type phase. © *1999 Elsevier Science Limited. All rights reserved*

Keywords: niobates, powders – solid state reaction, calcination, $FeNbO_4$, milling.

1 Introduction

The ultimate goal of ceramic processing is to achieve the desired phase(s), whilst keeping the sequence of steps as simple as possible. As is well known, both starting materials and processing history critically affect the properties of the final product, such that attention towards powder processing techniques is always required.

There is increasing interest in the use of some types of ABO_4 oxides, e.g. $FeNbO_4$, $FeTaO_4$ and $FeWO_4$, in gas sensor, catalytic and photodetector technologies. Moreover, the solid solution system $Fe(Nb_{1-x}W_x)O_3$ has been found to exhibit semiconducting and magnetic behaviour consistent with the coexistence of Fe^{2+} and Fe^{3+} ions. Electrical properties have been rationalised by an electron-hopping model, with magnetic behaviour signifying the low temperature dominance of antiferromagnetic exchange interactions for $0 \leq x \leq 0{\cdot}6$ and ferromagnetic interactions for $0{\cdot}7 \leq x \leq 1$.[1] As a dark brown oxide, iron niobate, $FeNbO_4$ is one of the well known compounds of the ABO_4 family, which has recently gained considerable attention.[2–10] This compound in particular has been investigated as a possible photoanode material, with potential applications in the conversion of solar energy.[3] Moreover, it is well known as the key precursor for the successful preparation of single-phase perovskite $Pb(Fe_{1/2}Nb_{1/2})O_3$ (PFN), which is becoming increasingly important for multilayer ceramic capacitor (MLCC) applications.[11]

In conventional mixed oxide routes to lead-based complex perovskite powders, second phases (chiefly pyrochlores) are readily introduced. For example, in the preparation of the well known relaxor, lead magnesium niobate (PMN), pyrochlore phases in the $PbO–Nb_2O_5$ system severely degrade the dielectric properties of the final product.[11] Similar problems of pyrochlore formation have been encountered in the fabrication of PFN powders, where the use of the precursor $FeNbO_4$ has been proposed as an effective way of producing PFN powder in high yield. This is analogous to the two-stage columbite route to PMN powder.[11] Interestingly, a two-stage mixed oxide route has also been employed with minor modifications in the synthesis of $FeNbO_4$ itself.[11,12] In general, production of single-phase $FeNbO_4$ is not straightforward, as minor concentrations of the phases $FeNb_2O_6$ and/or $Fe_4Nb_2O_9$ are sometimes formed alongside the major phase of Fe NbO_4.[3,10,13]

Much of the work concerning the $FeNbO_4$ compound has been directed towards determining polymorphs,[2,4,13] magnetic[5,6] and electrical[7,8]

*To whom correspondence should be addressed at present address: WBB Technology Ltd., Watts Blake Bearne & Co plc, Park House, Courtenay Park, Newton Abbot, TQ12 4PS, UK. Fax: +44-(0)1626-322386; e-mail: nthomas@wbb.co.uk

properties. Its polymorphism has been examined and described by a number of workers,[2,10,13,14] with four structural types identified:

1. a monoclinic structure in space group $P2/c$ (of wolframite-type), with an ordered distribution of Fe and Nb atoms; stable between 25 and 1085°C;
2. a monoclinic structure in space group C2/m (of $AlNbO_4$-type);[14]
3. an orthorhombic structure in space group *Pbcn* (referred to as the ixiolite[$MnTa_2O_6$] or α-PbO_2 type) with disordered cations; stable between 1085 and 1380°C;
4. a tetragonal structure in space group $P4_2/mnm$ (of rutile-type) with disordered cations; stable between 1380 and 1410°C.

Only limited attempts have been made to improve the yield of $FeNbO_4$ (FN) by optimising starting materials and processing steps. Whereas purity and reactivity are crucial, attention should also be given to the phase formation characteristics and processing-property relationships of this material, with a view to enhancing overall understanding. In this study, a modified mixed oxide synthetic route to FN has been employed, analogous to the synthesis of magnesium niobate, $MgNb_2O_6$ previously reported.[15]

2 Method

2.1 Powder preparation

FN powder was synthesised by the solid state reaction of reagent grade iron oxide Fe_2O_3 (99% purity) and niobium oxide Nb_2O_5 (99·9 + % purity), both supplied by Alfa (Johnson Matthey), according to eqn (1):

$$Fe_2O_3 + Nb_2O_5 \rightarrow 2FeNbO_4 \qquad (1)$$

Powder-processing was carried out as shown schematically in Fig. 1. The methods of mixing, drying, grinding, firing and sieving of the products were similar to those employed in the preparation of the columbite-like $MgNb_2O_6$, as described previously.[15]

Five calcination temperatures were selected to investigate the reaction to form iron niobate: 1050, 1075, 1100, 1125 and 1150°C, all for 4 h. Having established the optimum calcination temperature, alternative calcination times of 3, 4 and 5 h were applied at this temperature. For completeness, calcination times of 5 h at a temperature 25°C below and 2 h at 25°C above the optimum temperature were also investigated.

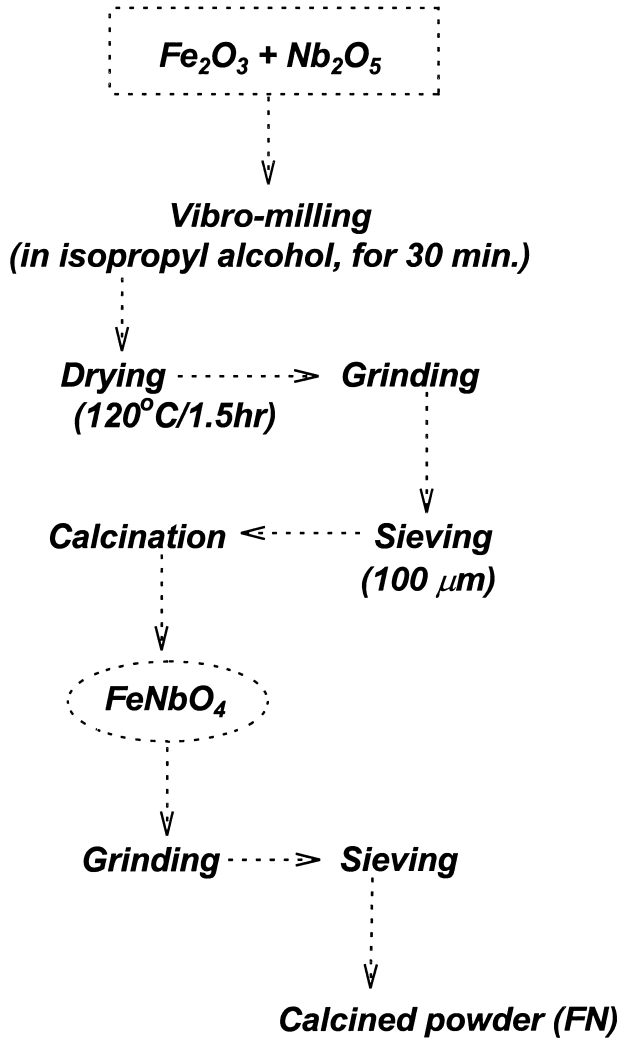

Fig. 1. Preparation route for the iron niobate $FeNbO_4$ powder.

2.2 Powder characterisation

Differential thermal analysis (DTA) (Perkin–Elmer, 7 Series Thermal Analysis System) was carried out in the temperature range from 600 to 1300°C. As-dried powder (100 mg) was placed into a platinum holder and measured at a heating rate of 10°C min^{-1} in air, with alumina powder as a reference. Calcined powders were examined by X-ray diffraction (CuK_α radiation), to identify the phases formed and optimum calcination conditions.

The particle size distributions of the samples were determined by laser diffraction techniques (MasterSizer, Malvern, UK). Powder morphologies and grain sizes were observed by scanning electron microscopy (Camscan SEM) interfaced to a digital image capture system. The chemical compositions and structures of the phases formed were elucidated by transmission electron microscopy (CM20 TEM/STEM operated at 200 keV) and energy-dispersive X-ray (EDX) analyser with an ultra-thin window. Powder samples were dispersed in solvent and deposited by pipette on to 3 mm holey carbon grids for observation by TEM.

3 Results and Discussion

3.1 Identification of the optimum calcination temperature for the formation of iron niobate

The DTA trace for the powder is given in Fig. 2, where the exothermic peak at 1198°C and the endothermic peak at 1240°C are shown. This does not show any direct relationship with earlier results concerning the formation of $FeNbO_4$.[2,10,13,14]

Powder XRD patterns of the calcined powders are given in Figs 3 and 4, respectively, with the corresponding JCPDS patterns also shown. The

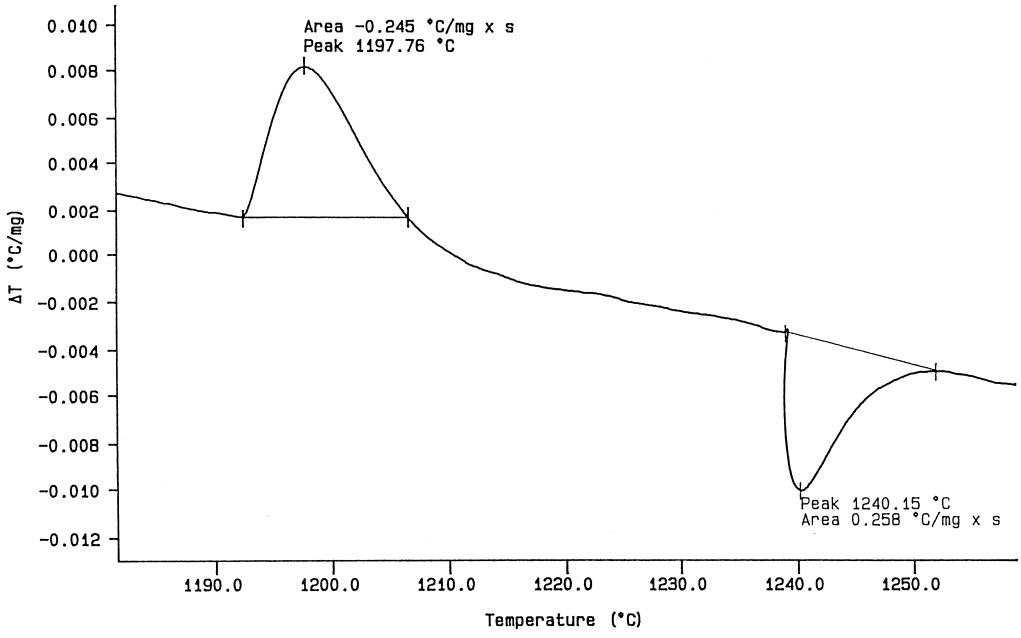

Fig. 2. A DTA curve for the $FeNbO_4$ powder.

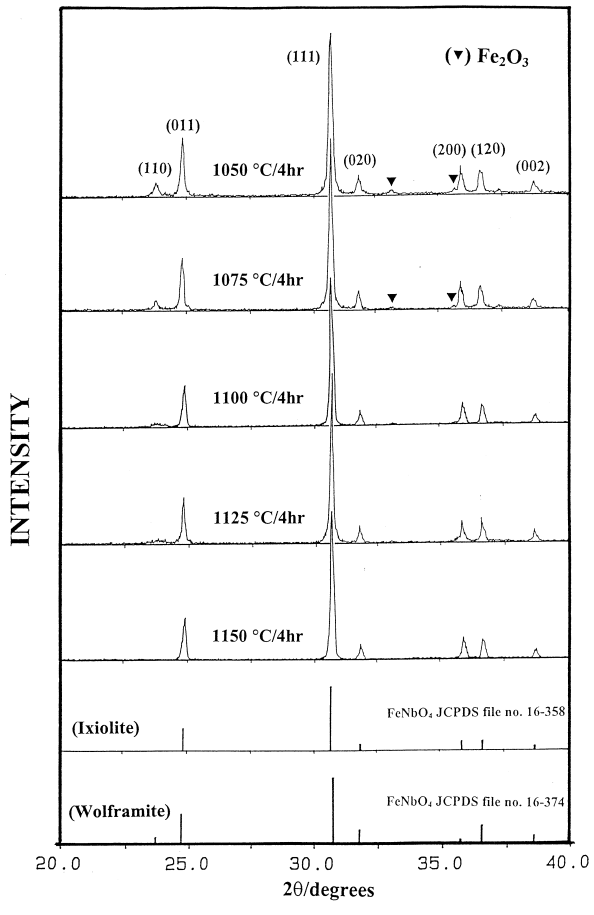

Fig. 3. Powder XRD patterns of the calcined powders at various calcination temperatures with constant dwell time.

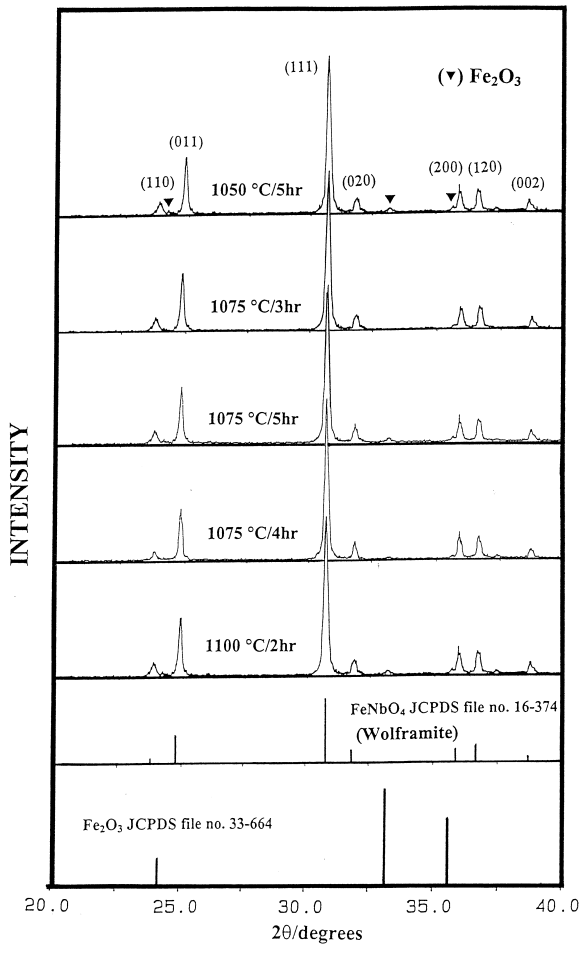

Fig. 4. Powder XRD patterns of the calcined powders at various calcination temperatures and times.

most obvious difference between the patterns for wolframite and ixiolite concerns the presence of an additional low-angle (110) peak for the former phase (Figs 3 and 5). The strongest reflections apparent in the majority of the XRD patterns indicate the formation of the iron niobate, $FeNbO_4$. These can be matched with JCPDS file numbers 16-374 and 16-358 for the monoclinic wolframite (Fig. 5) and orthorhombic α-PbO_2 phases (Fig. 6), respectively. It is seen that, with the exception of powders calcined at 1150°C, the wolframite phase is always present in the product. Moreover, some additional weak reflections are found in the XRD patterns (marked by ▼), which correlate with the precursor Fe_2O_3 (JCPDS file no. 33-664).

It may be concluded that, over a wider range of calcination conditions (1050–1150°C/4 h) than has been previously reported,[12,16,17] single phase

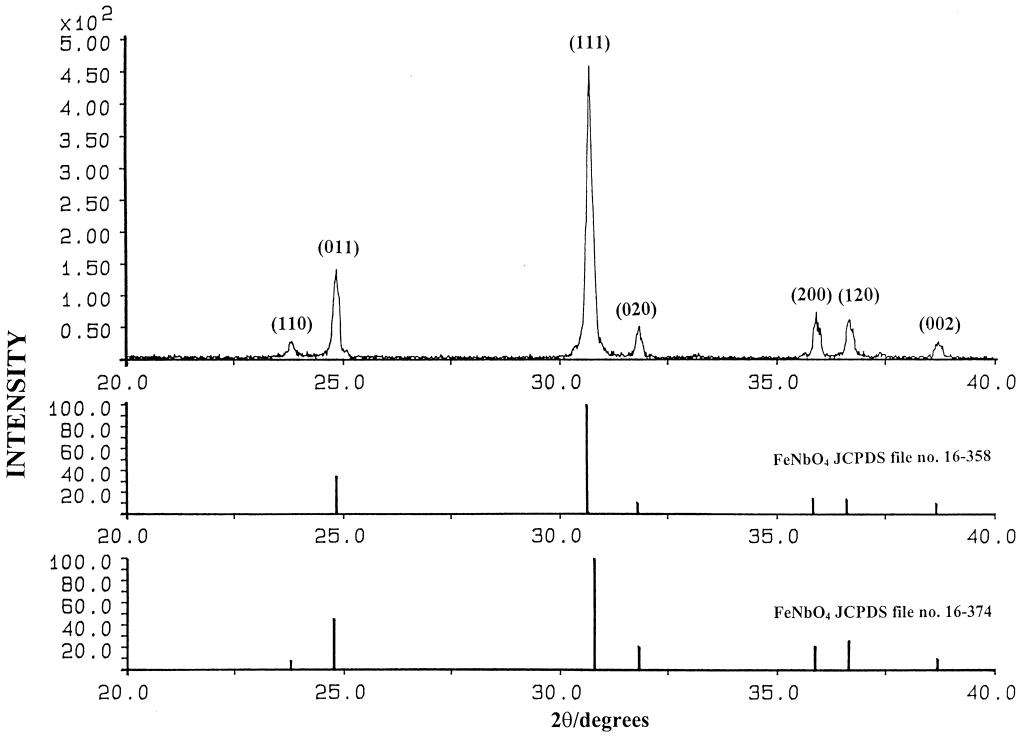

Fig. 5. Computerised JCPDS data-matching (file 16-374) confirms the formation of the wolframite-like phase $FeNbO_4$.

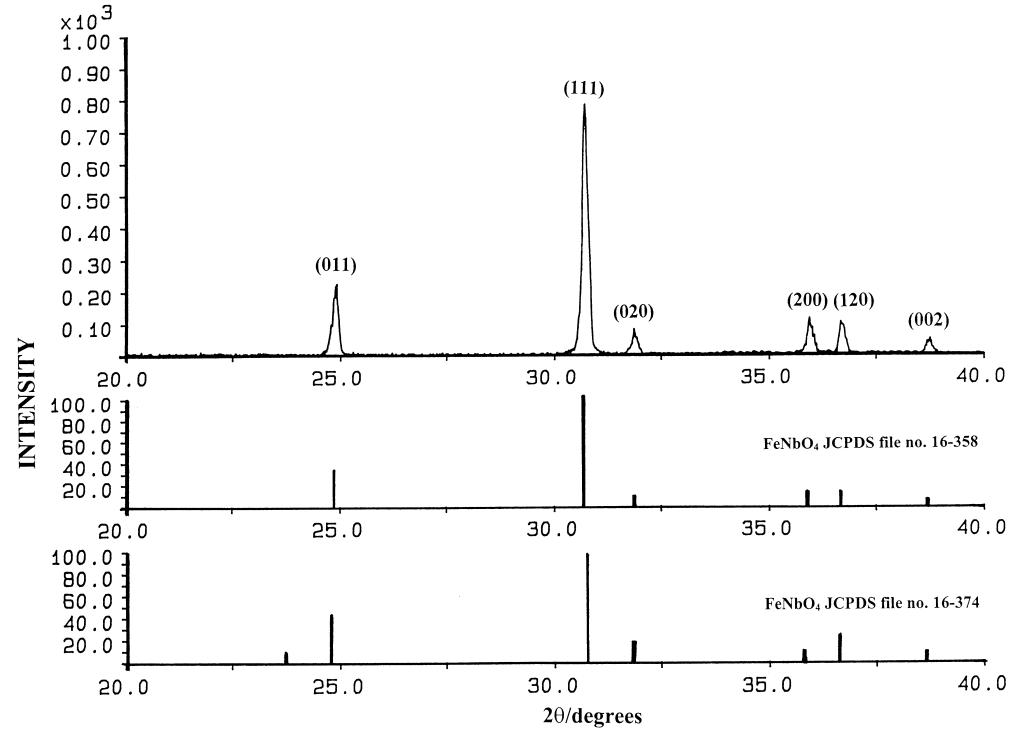

Fig. 6. Computerised JCPDS data-matching (file 16-358) confirms the formation of the ixiolite-like phase $FeNbO_4$.

$FeNbO_4$, in particular the low temperature wolframite phase, cannot be produced easily. In earlier work, formation of iron niobate has required long heat treatments, e.g. 1000°C/16 h,[4] 1000°C/192 h[8] for monoclinic $FeNbO_4$ and 800°C/72 h,[4] 1000°C/12 h,[7] 1000°C/24 h,[1] 1150°C/48 h,[3] 1200°C/24 h[5] and 1300°C/50 h[8] for orthorhombic $FeNbO_4$.

This study shows that a minor amount of the unreacted Fe_2O_3 phase co-exists along with the iron niobate $FeNbO_4$ phase, after calcination in the range 1000 to 1150°C. By increasing the calcination temperature, the yield of the monoclinic phase decreases significantly until at 1150°C, a single phase of orthorhombic $FeNbO_4$ is formed (Fig. 7). The relative proportions of $FeNbO_4$ and Fe_2O_3 quoted in Table 1 have been calculated according to the following approximate relationship, by analogy with our treatment of the yield of $MgNb_2O_6$ in a related synthesis:[15]

$$\text{wt\%FeNbO}_4\text{phase} = \left(\frac{I_{\text{FeNbO}_4}}{I_{\text{FeNbO}_4} + I_{\text{Fe}_2\text{O}_3}}\right) \times 100 \quad (2)$$

Here I_{FeNbO_4} and $I_{\text{Fe}_2\text{O}_3}$ refer to the intensities of the wolframite/ixiolite (111) and ferric oxide (104) peaks, respectively, these being the strongest reflections in both cases.

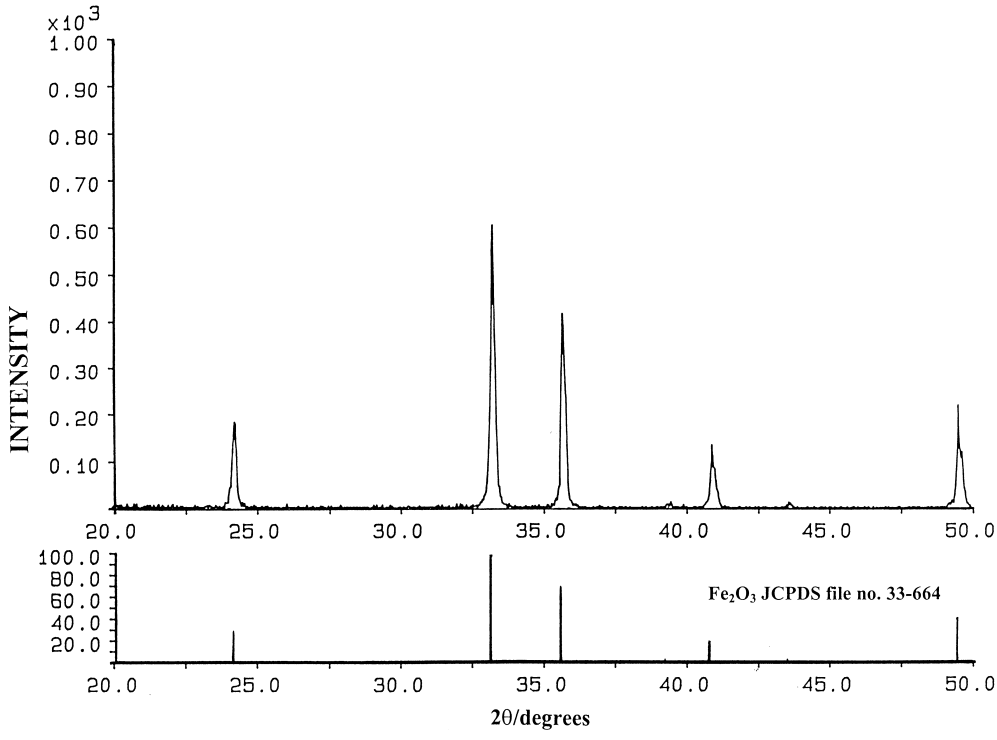

Fig. 7. Computerised JCPDS data-matching (file 33-664) confirms the phase composition of the starting precursor Fe_2O_3.

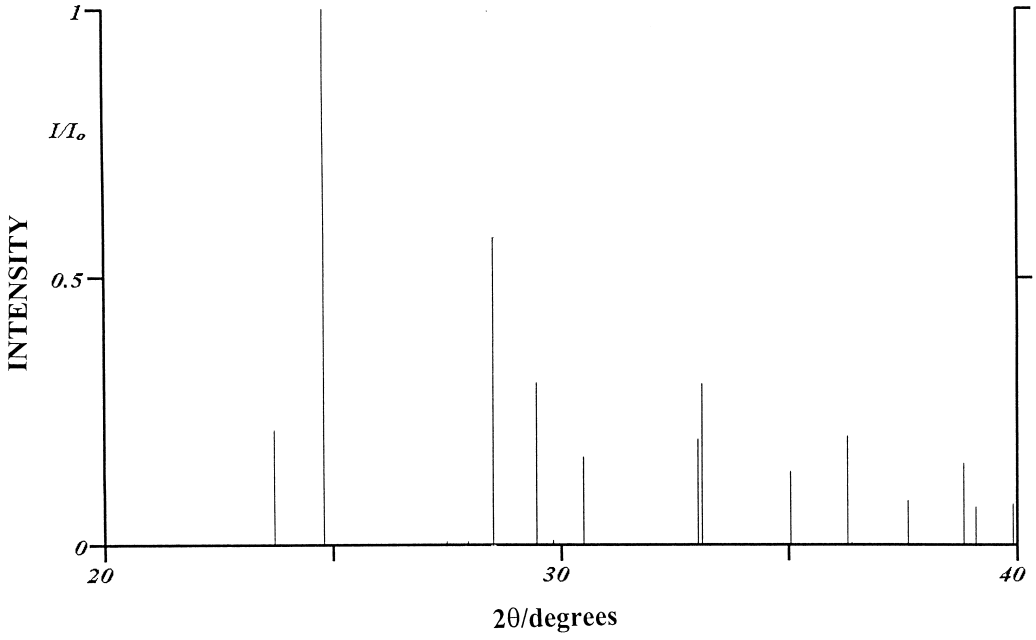

Fig. 8. Predicted XRD pattern of the monoclinic C2/m phase of $FeNbO_4$.

As might be expected, higher temperatures and different dwell times do not enhance the yield of the wolframite-like phase. Unlike the optimal calcination conditions reported earlier for single-phase wolframite $FeNbO_4$,[2] the implication of this work is that the monoclinic phase could best be produced by subsequent annealing at a temperature below 1085°C. This possibility has not been investigated, since the overriding objective is to synthesize single phase $FeNbO_4$, irrespective of the polymorph in which it is stabilized.

Table 1. Phase analysis for FN prepared by the modified oxide route

Sample	*Calcination conditions*		Qualitative concentrations of phases	
	Temperature (°C)	*time (h)*	*$FeNbO_4$ (wt%)*	*Fe_2O_3 (wt%)*
FN1	1050	4	96·6	3·4
FN2	1050	5	97·0	3·0
FN3	1075	3	100·0	0·0
FN4	1075	4	98·8	1·2
FN5	1075	5	97·2	2·8
FN6	1100	2	97·0	3·0
FN7	1100	4	99·2	0·8
FN8	1125	4	99·5	0·5
FN9	1150	4	100·0	0·0

The estimated precision of the concentration values for the two phases is ± 0·1%.

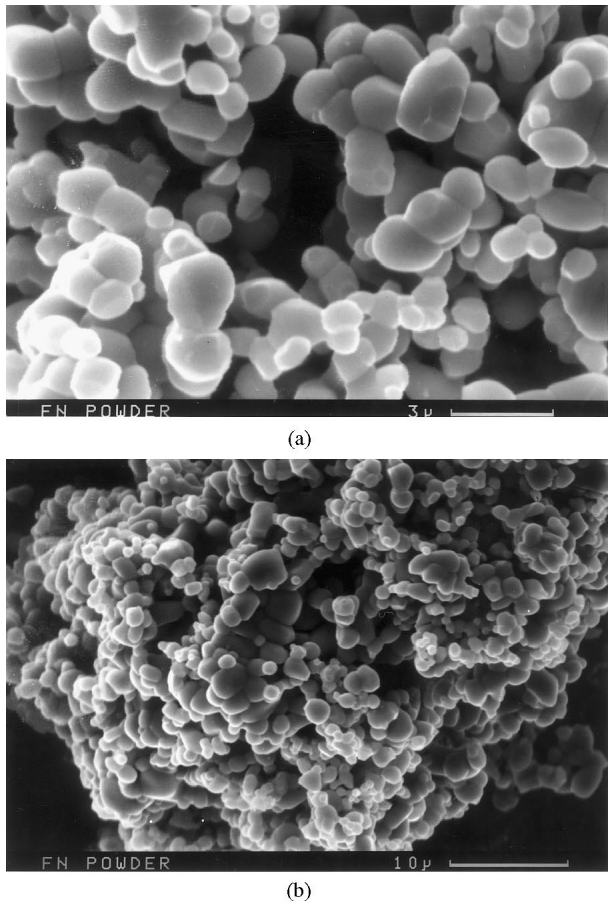

Fig. 10. SEM micrographs of the calcined $FeNbO_4$ powder.

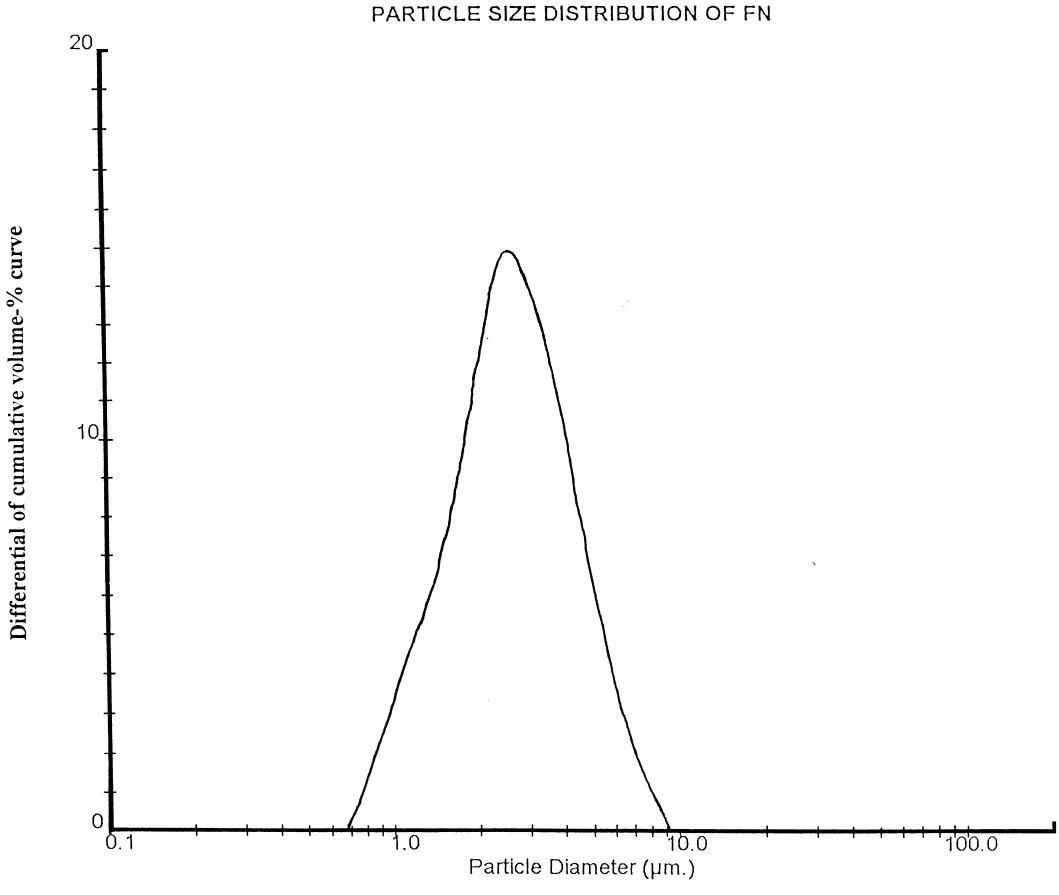

Fig. 9. The particle size distribution curve of the calcined $FeNbO_4$ powder.

It is also of interest to point out that no evidence has been obtained for the existence of the $AlNbO_4$-like monoclinic phase reported by Harder and Müller-Buschbaum.[14] As seen from a computed X-ray diffraction pattern of this phase (Fig. 8),[18] which has been generated from their published unit cell parameters and atomic coordinates, peaks such as that predicted at 28·5° do not occur in any of the patterns obtained experimentally.

3.2 Particle size analysis of $FeNbO_4$ powder

Figure 9 shows the particle size distribution curve of calcined orthorhombic $FeNbO_4$ powder, indicating an appreciable size fraction at about 2·5 μm within the possible range of 0·7 to 9·2 μm.

3.3 Microstructural analysis

SEM micrographs of the calcined $FeNbO_4$ powder (1150°C/4 h) are given in Fig. 10. The particles are agglomerated and basically irregular in shape. However, some spherical particles are clearly apparent at high magnification, ranging in diameter from 0·5–5·0 μm, in agreement with the particle size distribution previously given (Fig. 10). A TEM bright field image of discrete particles is shown in Fig. 11, indicating the particle sizes and shapes at higher magnification. The particle diameter was found to be about 0·5–1·5 μm in this TEM micrograph. By employing the selected area electron diffraction (SAED) technique, a second phase of rhombohedral Fe_2O_3 is identified (Fig. 12), in good agreement with the data in JCPDS file no. 33-664, from which the (003)–(101) interplanar angle is predicted to be 72·4°. Another minor phase is observed in Fig. 13, which correlates with a $FeNb_2O_6$ phase (JCPDS file no. 34–426), with a predicted $(10\bar{1})$–(121) interplanar angle of 96·4°. In general, EDX analysis using a 20 nm probe from a

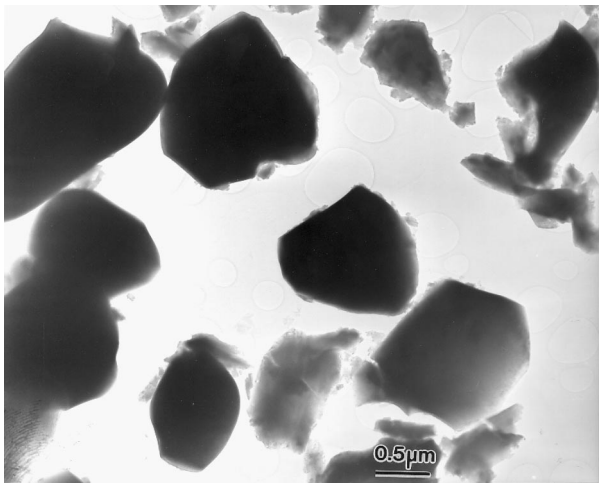

Fig. 11. TEM micrograph of the calcined $FeNbO_4$ powder.

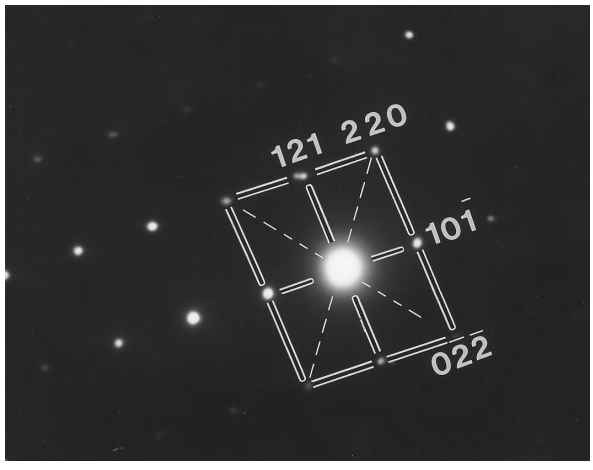

Fig. 13. SAED pattern of the columbite-like $FeNb_2O_6$ phase ($[1\bar{1}1]$ zone axis).

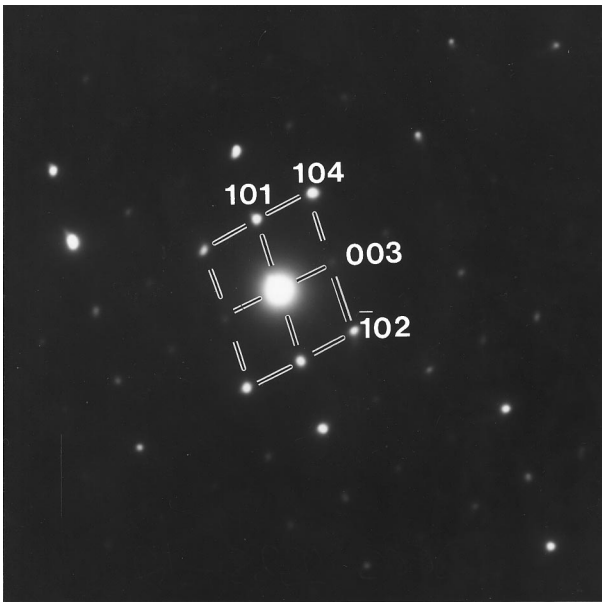

Fig. 12. SAED pattern of the rhombohedral Fe_2O_3 phase ([010] zone axis).

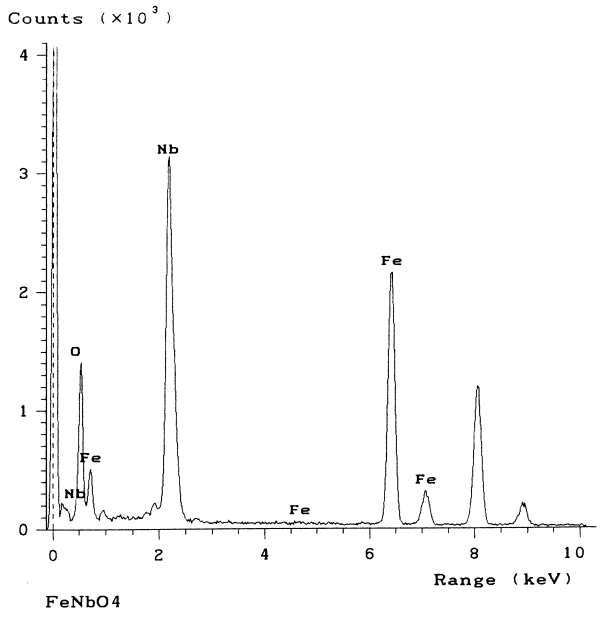

Fig. 14. EDX analysis of the calcined $FeNbO_4$ powder.

large number of particles of the calcined powder confirmed the composition to be $FeNbO_4$ (Fig. 14), in agreement with the XRD analysis.

4 Conclusion

Modified, mixed oxide synthetic routes for $FeNbO_4$ have been developed which show a high level of reproducibility. Evidence has been obtained for a 100% yield of orthorhombic $FeNbO_4$ at a calcination temperature of 1150°C. The preparative method involves the use of laboratory-grade precursors, low milling and drying times of powders, together with moderately low calcination temperatures and times. They represent significant time-savings compared to synthetic procedures currently advocated, and require only relatively impure laboratory-grade precursors.

Acknowledgements

One of the authors (S.A.) wishes to thank the DPST project and Thai Government for the financial support. Thanks are also due to Dr David Hind for helpful discussions on experimental technique.

References

1. Noda, Y., Shimada, M., Koizumi, M. and Kanamaru, F., Magnetic and electrical properties and Mössbauer effect in the solid solution $Fe(Nb_{1-x}W_x)O_4$ ($0 \leq x \leq 1$). *J. Solid State Chem.*, 1979, **28**, 379–384.
2. Roth, R. S. and Waring, J. L., Ixiolite and other polymorphic types of $FeNbO_4$. *Am. Mineral.* 1964, **49**, 242–246.
3. Koenitzer, J., Khazai, B., Hormadaly, J., Kershaw, R., Dwight, K. and Wold, A., Preparation and photoelectronic properties of $FeNbO_4$. *J. Solid State Chem.*, 1980, **35**, 128–132.
4. Pourroy, G., Lutanie, E. and Poix, P., Transition orthorhombic rutile in $xMFeO_4$–$(1-x)ZnF_2$ phases (M = Ta, Nb and $x > 0{\cdot}7$). *J. Solid State Chem.*, 1990, **86**, 41–49.
5. Harrison, W. T. A. and Cheetham, A. K., Structural and magnetic properties of $FeNbO_4$-II. *Mat. Res. Bull.*, 1989, **24**, 523–527.
6. Pourroy, G., Malats, I., Riera, I., Poix, P. and Poinsot, R., Low temperature syntheses of $NbFeO_4$ and $TaFeO_4$. influence of recrystallization on the magnetic properties. *J. Solid State Chem.*, 1990, **88**, 476–484.
7. Tena, M. A., Garcia-Belmonte, G., Bisquert, J., Escribano, P., Colomer, M. T. and Jurado, J. R., Impedance spectroscopy studies of orthorhombic $FeNbO_4$. *J. Mater. Sci.*, 1996, **31**, 2043–2046.
8. Schmidbauer, E. and Schneider, J., Electrical resistivity, thermopower, and ^{57}Fe Mössbauer study of $FeNbO_4$. *J. Solid State Chem.*,, 1997, **134**, 253–264.
9. Tena, M. A., Cordoncillo, E., Monros, G., Carda, J. and Escribano, P., Influence of Ti/Sn ratio and synthesis method in iron niobate doped with Sn and Ti. [$Fe_{0{\cdot}4}Ti_{0{\cdot}2-x}Sn_xNb_{0{\cdot}4}O_2$ solid solutions]. *Mater. Res. Bull.*, 1995, **10**, 943–945.
10. Laves, Von, F., Bayer, G. and Panagos, A., Structural relation between α-PbO_2, $FeWO_4$ (wolframite), and $FeNb_2O_6$ (columbite) and the polymorphism of $FeNbO_4$. *Schweiz. Mineral. Petrog. Mitt.*, 1963, **43**, 217–234.
11. Shrout, T. R. and Halliyal, A., Preparation of lead-based ferroelectric relaxors for capacitors. *Am. Ceram. Soc. Bull.*, 1987, **66**, 704–711.
12. Yasuda, N. and Ueda, Y., Dielectric properties of $PbFe_{1/2}Nb_{1/2}O_3$ under pressure. *Ferroelectrics*, 1989, **95**, 147–151.
13. Turnock, A. C., Fe-Nb oxides: phase relations at 1180°C. *J. Am. Ceram. Soc.*, 1966, **49**, 177–180.
14. Harder, M. and Müller-Buschbaum, Hk., $FeNbO_4$: Untersuchungen an Einkristallen mit Wolframit- und $AlNbO_4$-Struktur. *Z. anorg. allg. Chem.*, 1979, **465**, 99–105.
15. Ananta, S., Brydson, R. and Thomas, N. W., Synthesis, formation and characterisation of $MgNb_2O_6$ in a columbite-like phase. *Journal of the European Ceramic Society.* , 1999, **19**, 355–362.
16. Ichinose, N. and Kato, N., Dielectric properties of $Pb(Fe_{1/2}Nb_{1/2})O_3$-based ceramics. Jpn. J. Appl. Phys., 1994, **33**, 5423–5426.
17. Yasuda, N. and Ueda, Y., Temperature and pressure dependence of dielectric properties of $Pb(Fe_{1/2}Nb_{1/2})O_3$ with the diffuse phase transition. *J. Phys. Condens. Matter*, 1989, **1**, 5179–5185.
18. Thomas, N. W., *xrps X-ray Program Suite*, WBB proprietary software, Newton Abbot, UK, 1998.